CH-stretching Overtone Spectra of a Fast Rotating Methyl Group: 2-CH_3 and 2-CHD_2 Pyridines

D. Cavagnat* and L. Lespade

Laboratoire de Physico-Chimie Moléculaire, UMR 5803 CNRS, Université de Bordeaux I, 351 Cours de la Libération, F-33405 Talence Cedex France

Received: December 9, 2004; In Final Form: March 16, 2005

The CH-stretching overtone spectra of the methyl group in gaseous 2-CH_3 and 2-CHD_2 methylpyridines are recorded with conventional Fourier transform near-infrared spectroscopy in the $\Delta v_{CH} = 1-4$ regions and by intracavity laser photoacoustic spectroscopy in the $\Delta v_{CH} = 5$ and 6 regions. All spectra exhibit a complex structure. They are analyzed with a theoretical model that incorporates, within the adiabatic approximation, the coupling of the anharmonic CH-stretch vibrations described by Morse potentials with the quasifree internal rotation of the methyl group and with isoenergetic combination states involving the six angle deformation modes of the methyl group. The molecular vibrations are calculated in terms of redundant internal coordinates in an unambiguous canonical form. A simultaneous analysis of different isotopic derivatives is thus achieved. The Fermi resonance coupling parameters are those previously determined for toluene. The technique of diabatic rotations is used to disentangle the multiple avoided crossings occurring along the internal rotation coordinate θ in the calculated spectra, which become rapidly very dense owing to the low symmetry of the system. This simulation is successful in reproducing the experimental spectra. In addition, the transferrability of the Fermi resonance coupling parameters between two parent molecules is demonstrated.

I. Introduction

Intramolecular vibrational energy redistribution (IVR) and its effects on chemical reactivity has been the subject of several studies during these past decades. IVR has been shown to be a highly structured process mainly controlled by the coupling of a bright state to a small subset of possible dark background states. This suggests that the density of states that actually controls IVR depends on the pattern of vibrational resonances resulting from bond connectivity and anharmonicity.[1] Short time resonance dynamics can thus be to some extent characteristic of functional groups. Thus, chromophore-specific interactions may be transferrable between molecules containing these functional groups.[2−5] Obtaining such predictability would represent non-negligible progress for the analysis of the IVR phenomena in large organic molecules.

However, only few functional groups with characteristic IVR dynamics have been so far investigated in detail.[2−5] For example, the well-known methyl stretch−bend coupling, principally analyzed in small molecules, should exist in all methyl-containing molecules.[2,6−17] However, its role in the IVR of the CH stretch of the methyl group can be different for each molecule, depending on the strength of coupling and tuning into resonance, factors largely dependent on the molecular environment of the methyl group.[14−17]

Similarly, the dependence of IVR on structural changes or large-amplitude motion has been related to the chromophore concept.[2−5,12,15−19] The large coupling terms between the coordinate of a highly anharmonic large-amplitude motion and the other molecular coordinates can contribute, alone or simultaneously with Fermi resonances, to the IVR observed in these systems.[15−17,20−24] For instance, molecules possessing almost freely rotating methyl rotors exhibit IVR acceleration effects in excited electronic states.[25] However, there is no clear indication of such an enhancement in the ground electronic state,[4,5,15−17,19] contrary to what is observed when a skeletal torsional mode is present.[18] The study of these methylated molecules should thus yield additional insight into the role played by internal dynamics in IVR. The analysis of the CH-stretching overtone spectra of these relatively large systems is however rather intricate, even at low energy in the gas phase, because they generally exhibit complex and broad features.[15−17,22−24]

In our previous works, the CH-stretching vibrational overtone spectra of the almost freely rotating methyl group of nitromethane[15] and toluene[16] have been analyzed with a model taking into account simultaneously (in contrast to similar studies[12,17,22−24]) the Fermi resonance couplings and the coupling with internal rotation. In these compounds, the coupling of the CH vibrator with internal rotation determines to a large extent the methyl CH-stretching overtone profiles. However, especially in toluene, some of these spectra are strongly perturbed by a fast intramolecular vibrational energy redistribution because of Fermi resonances. This phenomenon arises only in limited energy domains. Indeed, the frequencies of the vibrations (CH_3 deformations) which can enter into resonance with the CH-stretching bright states are essentially within two energy domains (typically around 1400 and 1000 cm^{-1}). Some "lack of tuning" can thus occur when these "doorway" combination states are not in resonance with the bright states, in contrast to what happens generally with CH_2 methylene groups.[26]

The study of 2-, 3- or 4-methylpyridines allows investigation of the evolution of methyl CH-stretching band profiles with increasing barrier height and increasing lack of potential symmetry. In previous papers, some spectral changes have been ascribed to differences in the symmetry and magnitude of the internal rotation barrier of the methyl group.[17,24] None of these

* Author to whom correspondence should be addressed. E-mail: d.cavagnat@lpcm.u-bordeaux1.fr.

10.1021/jp044399f CCC: $30.25
Published on Web 04/15/2005

studies have considered the possible perturbation of the spectral profiles by the CH stretch−bend Fermi resonance. Contrary to what is observed for the first CH-stretching overtones ($\Delta v = 1-3$) of the $-\alpha d_2$ derivatives,[17] the fundamental CH-stretching spectra of $-\alpha d_0$ methylpyridines are largely affected by a strong CH stretch−bend Fermi resonance phenomenon,[27] very similar to that observed in $-\alpha d_0$ toluene.[16] In the higher excited states, this IVR pathway cannot be disregarded; it could actually contribute to the differences observed between the methyl profiles of $-\alpha d_0$ and $-\alpha d_2$ methylpyridine derivatives.[24]

In the present study, we analyze the methyl CH-stretching overtone spectra of the 2-methylpyridine, which possesses a 3-fold hindering rotational barrier of the methyl group (91 cm^{-1} in the gas phase as determined by microwave[28]). As done previously,[16] we have tried to reproduce the CH-stretching spectra of the methyl group of both 2-CH_3 and 2-CHD_2 methylpyridine derivatives with a single set of parameters, which takes into account the coupling with the internal rotation and the Fermi resonance couplings. Furthermore, we have used the Fermi resonance coupling parameters previously determined for toluene.

This study has two principal aims: (i) to check the transferrability properties of the IVR parameters for methyl groups belonging to related molecules and (ii) to analyze how the IVR processes are affected by the height and symmetry of the methyl-hindering potential of the methyl group. The comparison of these results with the ones obtained for similar molecules (nitromethane,[15] toluene[16]), may help to elucidate the IVR mechanisms associated with almost freely rotating methyl groups.

The present paper is organized as follows: after the presentation of the experimental details, we recall the theoretical model which takes into account the two principal couplings likely to affect the CH-stretching overtones. The overtone spectra of the two isotopic derivatives of 2-methylpyridines are then presented and analyzed in the light of those obtained for toluene.

II. Experimental Section

Perhydrogenated 2-methylpyridine (99%) was purchased from Aldrich. The product was dried and degassed by the freeze−pump−thaw method.

The isotopic derivatives 2-αd_2 methylpyridine and 2-αd_2, 6-d_1 methylpyridine (in this later compound, the lower-frequency aryl CH-stretching mode vanishes allowing a better observation of the methyl CH-stretching spectra) were synthesized and purified according to the procedure described in ref 17c. The isotopic purity, as checked by mass spectrometry, was 95%. The products were transferred into the different measurement cells using a vacuum line.

The near-infrared spectra ($\Delta v = 1-4$) were recorded between 2800 and 12 000 cm^{-1} with a resolution ranging between 0.5 and 2 cm^{-1} on a BioRad FTS-60A spectrometer. A homemade cell ($l = 10$ cm) and an Infrared Analysis long path minicell ($l = 1-7.2$ m) equipped with CaF_2 windows were used.

The visible spectra ($\Delta v = 5$ and 6) were recorded with a homemade intracavity photoacoustic spectrometer previously described.[15−16] A Coherent Innova 70 Ar^+ laser was used to pump a CR599 dye laser fitted with high-reflectance optics for 2-pyridine (13 000−14 500 cm^{-1}) and DCM (15 200−16 300 cm^{-1}) dyes. The laser bandwidth was 1 cm^{-1} and the wavenumber difference between successive data points was typically 0.7 cm^{-1}. Each point record was accumulated 800 times.

The spectra of 2-methylpyridine were recorded under vapor pressure (typically 11 mmHg at room temperature).

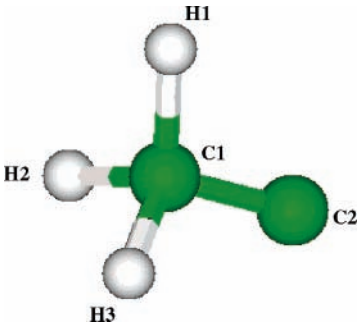

Figure 1. Methyl group of 2-methylpyridine (C_1 is the carbon atom of the methyl group, C_2 that of the pyridine ring). The coordinates used in the calculations are defined as: $r = CH_1$, $r' = CH_2$, $r'' = CH_3$, $\alpha = H_2CH_3$, $\alpha' = H_1CH_3$, $\alpha'' = H_1CH_2$, $\beta = H_1C_1C_2$, $\beta' = H_2C_1C_2$, $\beta'' = H_3C_1C_2$. The internal rotation angle of the methyl group $\theta = 0$ when the CH_1 bond is in the pyridine ring plane on the opposite side of the N atom.

III. Theoretical Approach

The coupling between the vibrational motions and the large-amplitude internal rotation is modeled by the total Hamiltonian $H_T = H_{v-r} + H_r$. The difference between the time scales of the internal rotation θ and the vibrational motions q_i allows solution of the Schrödinger equation in the adiabatic approximation.[12,15−17,22] This leads to a system of two equations describing (i) the molecular vibrations (q_i) for each θ value and (ii) the large amplitude motion where the vibrational energy $e(\theta)$ acts as an additional potential. The coordinate of the methyl internal rotation θ is defined as the angle between the plane formed by the pyridine ring and CH_1 (Figure 1)

$$H_{v-r}(q_i,\theta)\,\varphi(q_i,\theta) = e(\theta)\,\varphi(q_i,\theta)$$
$$[H_r(\theta) + e(\theta)]\,\psi(\theta) = E\psi(\theta) \quad (1)$$

$$\frac{H_r(\theta)}{hc} = -\frac{d}{d\theta}B_v(\theta)\frac{d}{d\theta} + \frac{1}{2}V_3(1-\cos 3\theta) + \frac{1}{2}V_6(1-\cos 6\theta) \quad (2)$$

$V_0(\theta) = (1/2)V_3(1 - \cos 3\theta) + (1/2)V_6(1 - \cos 6\theta)$ is the rotational potential determined by microwave studies.[28] $B_v(\theta)$ is the reduced rotational constant of the methyl rotor about the methyl top axis. Owing to the medium resolution used in our measurements, B_v has been determined from the geometrical changes of the methyl group, i.e., the CH bond length increase (the top angle change being disregarded):[29] $B_v = B_e - \alpha(v + 1/2)$ ($B_e = 5.4893$ cm^{-1} and $\alpha = 0.05$ cm^{-1} for CH_3, $B_e(\theta) = 3.3678 + 0.0032\cos\theta - 0.005\cos 2\theta$ cm^{-1}, $\alpha = 0.01$ cm^{-1} for CHD_2).

In the ground vibrational state, the effective potential of the internal rotation of the methyl group depends on the molecular energy.

$$V_{\text{eff}}(\theta,0) = V_0(\theta) + \frac{1}{2}\sum_i e_i(\theta) \quad (3)$$

As determined before by ab initio methods, the zero-point vibrational energy (ZPVE) of the other (3N-7) vibrations ($(1/2)\sum_i e_i(\theta)$), is independent of θ for the CH_3 methyl group and displays a θ variation of: $-2.4\cos\theta + 17.7\cos 2\theta + 8.7\cos 3\theta + 0.3\cos 4\theta$ cm^{-1} for the CHD_2 methyl group.[17c]

When the CH-bond stretch is excited with v quanta of energy, the effective potential of the methyl internal rotation is increased

by the corresponding vibrational part $e_{CH}(\theta)$:

$$V_{eff}(\theta,\upsilon) = V_{eff}(\theta,0) + e_{CH}(\theta) \quad (4)$$

Because of the complexity of the vibrational problem, only the modes likely to be involved in Fermi resonances with the CH bond-stretching overtones up to $\Delta\upsilon = 6$ are considered for the calculation of $e_{CH}(\theta)$. This vibrational energy part $e_{CH}(\theta)$ is calculated using nine internal curvilinear coordinates of the methyl group, namely the displacement coordinates of the three CH/CD bonds (r), of the three HCH/HCD angles and of the three HCC/DCC angles deformations (α). As previously stated,[30] this set of internal coordinates offers a powerful tool to test the physicochemical meaning of the force constants. They also allow transferrability and interpolation of the force fields between related molecules. As previously done,[16] the redundancy between the six angles is removed by using the unambiguous formalism described by Martinez Torres at al.[31] To test the transferrability of the Fermi resonance coupling terms between systems possessing a fast rotating methyl group, we have used the Fermi resonance coupling constants deduced from the toluene study.[16] Only the variation of these parameters versus the internal rotation coordinate has been adapted to the symmetry of the system.

The effective vibrational Hamiltonian, expanded up to third order, is written as the sum of four terms:

$$H = H^0 + H^1 + H^2 + H^3 \quad (5)$$

The zero-order Hamiltonian, H^0, describes the pure stretching and bending vibrations of the methyl group considered, respectively, as weakly coupled Morse oscillators and weakly anharmonic modes.

$$\frac{H^0}{hc} = \sum_i^3\sum_j^3 \left\{\frac{1}{2}g^0_{r_ir_j}p_{r_ir_j} + D_i[1 - e^{-a_i(\theta_i)r_i}]^2\right\} + \sum_i^3\sum_{j\neq i}^3 \left\{\frac{1}{2}f_{r_ir_j}(\theta'_{ij})r_ir_j\right\} + \sum_i^6\sum_j^6 \left\{\frac{1}{2}(g^{0*}_{\alpha_i\alpha_j}p_{\alpha_i}p_{\alpha_j} + f^*_{\alpha_i\alpha_j}(\theta_{ij})\alpha_i\alpha_j + f^*_{\alpha_i\alpha_i\alpha_i}(\theta_{ii})\alpha_i^3 + f^*_{\alpha_i\alpha_i\alpha_i\alpha_i}(\theta_{ii})\alpha_i^4)\right\} \quad (6)$$

r_i are the bond displacement coordinates ($r_1 = r_{CH_1}$, $r_2 = r_{CH_2}$, $r_3 = r_{CH_3}$), D_i the dissociation energy of the CH bond and $a_i(\theta)$ the Morse potential parameters. They are related to the harmonic wavenumber ϖ_0 and to the anharmonicity χ. Their dependence on the internal rotation coordinate θ is directly linked to the variation of $\varpi_0(\theta)$ determined by ab initio calculations. α_i are the valence angle displacement coordinates (α_1, α_2, α_3 correspond to the HCH or HCD angles, α_4, α_5, α_6 to the HCC or DCC angles) (Figure 1). θ_i is equal to θ for $i = 1$ and 4, $\theta + 2\pi/3$ for $i = 2$ and 5, and $\theta + 4\pi/3$ for $i = 3$ and 6, with $\theta = 0$ when the CH_1 bond is in the pyridine ring plane in trans position versus the N atom. θ'_{ij} is the angle between the molecular plane and the bisector of the angle between the two bonds r_i and r_j, θ_{ij} the angle between the molecular plane and the bisector of the sum of the angles α_i and α_j ($i \neq j$), and θ_{ii} the angle between the molecular plane and the bisector of the angle α_i. g* and f* are the canonical kinetic energy matrix term and the canonical force field matrix term, respectively.[31]

H^1, H^2, and H^3 correspond to the first, second, and third order in the Taylor series expansion of the elements $g_{\alpha\alpha}$ of the Wilson G matrix[32] in the displacement coordinates about the equilibrium configuration. Only the most important terms of the kinetic energy are retained. The corresponding potential energy terms are added.

H^1 contains the Fermi resonance terms between stretching and bending states, H^2 and H^3 give some higher-order interaction terms between stretches and bends:

$$\frac{H^1}{hc} = \frac{1}{2}\sum_{k=1}^3\sum_{i=1}^6\sum_{j=1}^6 \left\{\left(\frac{\partial g^0_{\alpha_i\alpha_j}}{\partial r_k}\right)^*_e r_k p_{\alpha_i}p_{\alpha_j} + \left(\frac{\partial g^0_{r_k\alpha_i}}{\partial \alpha_j}\right)^*_e p_{r_k}\alpha_j p_{\alpha_i} + f^*_{r_k\alpha_i\alpha_j}(\theta_k)r_k\alpha_i\alpha_j\right\} \quad (7)$$

$$\frac{H^2}{hc} = \frac{1}{4}\sum_{k=1}^3\sum_{i=1}^6\sum_{j=1}^6 \left\{\left(\frac{\partial^2 g^0_{\alpha_i\alpha_j}}{\partial^2 r_k}\right)^*_e r_k^2 p_{\alpha_i}p_{\alpha_j} + f^*_{r_k}r_k\alpha_i\alpha_j(\theta_k)r_k^2\alpha_i\alpha_j\right\} \quad (8)$$

$$\frac{H^3}{hc} = \frac{1}{12}\sum_{k=1}^3\sum_{i=1}^6\sum_{j=1}^6 \left\{\left(\frac{\partial^3 g^0_{\alpha_i\alpha_j}}{\partial^3 r_k}\right)^*_e r_k^3 p_{\alpha_i}p_{\alpha_j} + f^*_{r_kr_kr_k\alpha_i\alpha_j}(\theta_k)r_k^3\alpha_i\alpha_j\right\} \quad (9)$$

To calculate the energy, the effective Hamiltonian of eq 5 is expanded in a basis of functions that are the products of Morse oscillator functions for the CH/CD bond stretches and harmonic oscillator wave functions for the bends. When the zero-point energy is subtracted, the diagonal elements of the Hamiltonian expansion lead to the unperturbed energies:

$$\sum_i^3 \{(\varpi^0_{r_i}(\theta_i) - \bar{\chi}_{r_i}(\theta_i))\upsilon_{r_i} - \bar{\chi}_{r_i}(\theta_i)\upsilon^2_{r_i}\} + \sum_i^6 \{(\varpi^0_{\alpha_i}(\theta_{ii}) - \bar{\chi}_{\alpha_i}(\theta_{ii}))\upsilon_{\alpha_i} - \bar{\chi}_{\alpha_i}(\theta_{ii})\upsilon^2_{\alpha_i}\} - \sum_i^3\sum_{j\neq i}^3 \bar{\chi}_{r_i\alpha_j}(\upsilon_{r_i},\theta_i)\upsilon_{\alpha_j} - \sum_i^3 \bar{\chi}_{r_i\alpha_{i+3}}(\upsilon_{r_i},\theta_i)\upsilon_{\alpha_{i+3}} \quad (10)$$

υ_r and υ_α are the quantum numbers in bonds stretch and bend motions, respectively. $\varpi^0_r(\theta)$, $\varpi^0_\alpha(\theta)$, $\bar{\chi}r(\theta)$, and $\bar{\chi}_\alpha(\theta)$ are displayed in Table 1 (the fitted potential parameters of the pure bending modes are given not in terms of $f_{\alpha\alpha\alpha}$ and $f_{\alpha\alpha\alpha\alpha}$ of eq 6 but as $\bar{\chi}_\alpha(\theta)$, which is mass dependent) The cross anharmonicities are defined by the relationship:

$$\bar{\chi}_{r\alpha}(\upsilon_r,\theta) = \left\{\left\langle \upsilon_r\left|\frac{H^1}{hc}\right|\upsilon_r\right\rangle + \left\langle \upsilon_r\left|\frac{H^2}{hc}\right|\upsilon_r\right\rangle + \left\langle \upsilon_r\left|\frac{H^3}{hc}\right|\upsilon_r\right\rangle\right\} \quad (11)$$

To model the experimental spectra, the Schrödinger equation for the υth manifold, expressed in matrix form, is solved by diagonalization of the Hamiltonian matrix $\boldsymbol{H}$:

$$\sum_j H_{ij}(\theta)c_{jm}(\theta) = hc\varpi_m(\theta)c_{im}(\theta) \quad (12)$$

The resulting eigenvalues $\varpi_m(\theta)$ and eigenvector elements $c_{im}(\theta)$ are calculated for different values of the methyl internal rotation angle θ varying from 0 to 180° in steps of 3°.

The θ variations of the vibrational energy for each of the most intense $\varpi_m(\theta)$ and for the corresponding coefficients $c_{im}(\theta)$ are then determined and added to $V_{eff}(\theta,0)$ (eq 4) to obtain the $V^m_{eff}(\theta,\upsilon)$ corresponding to the υth polyad.

Even though toluene and 2-methylpyridine have similar molecular sizes, the lower symmetry of 2-methylpyridine implies

a higher probability of anharmonic couplings between the vibrational states. Thus, the active density of states is increased and the vibrational energy can be widely spread. Furthermore, as expected even in a reduced dimensional molecular Hamiltonian where large amplitude motion is treated adiabatically as a reaction path,[33] the frequencies of two or more modes can cross each other along the large amplitude motion coordinate (θ). This introduces highly oscillatory components in the parametric dependence of the eigenfunctions on the channel coordinate θ. Actually, it is increasingly (already at $v \geq 4$) difficult to follow correctly the θ variation of the calculated perturbed vibrational states that exhibit several (avoided) crossings. To disentangle this complex pattern of vibrational states, we have used the technique of diabatic rotations developed by Luckhaus.[33b] This method, applied by the author to a full dimensional vibrational calculation[33b] and extended to an approximate harmonic reaction path Hamiltonian,[33a] allows an efficient deperturbation of multiple avoided crossings in dense vibrational spectra of complex systems. The diabatic rotations allow a systematic construction of locally diabatic channels.

The energies and the wave functions of the internal rotational states associated with the ground vibrational state (all $v_i = 0$) and with the vth polyad are calculated by solving the Schrödinger eq 1 with the corresponding effective potentials on a basis set of 85 free rotors. The CH-stretching overtone spectra are then reconstructed by adding the CH transitions calculated between the energy levels of the potentials $V_{\text{eff}}(\theta,0)$ and $V^m_{\text{eff}}(\theta,v)$. Because for each θ value the mode intensities inside each polyad are assumed to come from the CH bond-stretching overtones and because $\varphi(r_i,\theta)$ depends slowly on θ (adiabatic approximation), the dipole moment function of the methyl group for each retained ϖ_m mode is written:

$$\mu^j_m(\theta) = \sum_i^3 \sum_n^4 c_{im}(\theta)\mu^j_{ni}(\theta) \int \varphi^*_v(r_i,\theta) r_i^n \varphi_0(r_i,\theta) \mathrm{d}r_i \quad (13)$$

$c_{im}(\theta)$ is the θ variation of the intensity coefficient corresponding to the CH_i bond for the ϖ_m mode. The integrals of eq 13 are the matrix elements over the Morse oscillator wave functions. $\mu^j_{ni}(\theta)$ is the θ variation of the dipole moment derivatives at the nth order ($n = 1-4$) associated with the CH_i bond ($j = x$, y, z represents the three principal molecular axes; xz determines the molecular plane with z collinear to the CC bond and y perpendicular to the molecular plane). These dipole moment functions are obtained from ab initio calculations as Taylor series expansion in the CH stretching and as Fourier series expansion for the internal rotation coordinates.[17b]

The infrared intensity of the CH-stretching transitions between two states, $|0,k\rangle \rightarrow |v,k'\rangle$, ($|0,k\rangle$, and $|v,k'\rangle$ being respectively the kth and k'^{th} internal rotation levels in the ground and excited vibrational states) is given by the expression (P being the Boltzmann factor):

$$I_{|v,k'\rangle \leftarrow |0,k\rangle} = \upsilon_{vk',0k}\, P \sum_j^3 \left(\int \Psi^*_{vk'}(\theta)\mu^j_m(\theta)\Psi_{0k}(\theta)\mathrm{d}\theta\right)^2 \quad (14)$$

Any interaction between the internal rotation and the rotation of the entire molecule is neglected because of the difference between rotational constants. The effect of the overall rotation is taken into account by convoluting each transition with the theoretical asymmetrical top vibration−rotation profile corresponding to each component of the spectrum (A, B, or C type, depending on whether the transition involves the μ^z, μ^x, or μ^y dipole component).[34] The observed broadening of the bands

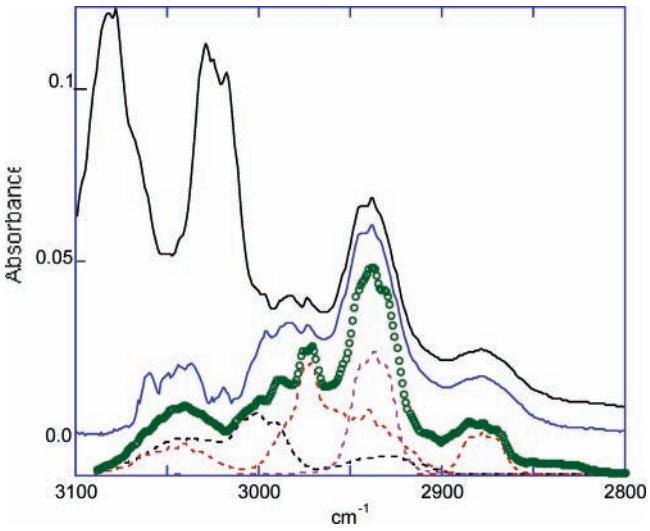

Figure 2. Experimental spectra without (offset upper solid line) and after subtraction of the aryl CH bands (middle solid line) and the calculated (circle line) spectrum in the $\Delta v = 1$ CH-stretching region of gaseous 2-$CH_3C_5NH_4$ at 298 K. The experimental spectrum is obtained by FTIR with a 10-cm path-length cell, a pressure of 11 Torr, and a resolution of 0.5 cm^{-1}.

(which may be due to the increase of the density of states weakly coupled to the CH bond as the vibrational molecular energy increases) is modeled by convoluting these profiles with a Lorentzian the half-width of which is adjusted for each overtone.

The calculated spectra for all the ϖ_m for which c_{im} is not negligible are then added to yield the vibrational ($v - 1$)th overtone spectrum.

IV. Results and Discussion

The different parameters used in this calculation and their θ variation are displayed in Tables 1 and 2.

Most of the parameter values in Table 1 are spectroscopically scaled ab initio values. The values of $\varpi^0_r(\theta)$ and of $\bar{\chi}_r(\theta)$ (Table 1) are slightly different from the ones previously determined.[17c,24b] This can be ascribed to a more precise determination of these values when all the coupling parameters are taken into account. In particular, the $\bar{\chi}_r(\theta)$ value is now equal to -58 cm^{-1}, the usual value for a methyl group.[2,14−16] The CH interbond coupling $\lambda_{rr}(\theta)$ value -20.1 cm^{-1} is very similar to that of toluene.[16] The θ dependence of the harmonic bending $\varpi_\alpha(\theta)$ and rocking $\varpi_\beta(\theta)$ frequencies and the effective interaction force constants between the HCH ($\alpha = \alpha_1$, $\alpha' = \alpha_2$, $\alpha'' = \alpha_3$) and HCC ($\beta = \alpha_4$, $\beta' = \alpha_5$, $\beta'' = \alpha_6$) deformation angles of the methyl group are parametrized to reproduce the ab initio variations of the bending and rocking normal modes of the methyl group (Tables 3 and 6). The anharmonicity constants $\bar{\chi}_\alpha(\theta)$ and $\bar{\chi}_\beta(\theta)$ cannot be accurately determined and are constrained to the same value (-5 cm^{-1}) as that used in the toluene study.[16] The same Fermi resonance parameters as those calculated for toluene[16] are used with only the θ variation adapted to the lower symmetry of the present system (Table 2).

(a) CH_3 Derivative. The $\Delta v = 3-6$ methyl CH-stretching spectra of this compound have been previously studied and analyzed by considering only the coupling between the CH stretch and the internal rotation of the methyl group.[24a,b]

As seen in Figures 2−7, which show the experimental and calculated CH-stretching overtone spectra of vapor phase 2-$CH_3C_5NH_4$ at room temperature, Fermi resonance couplings cannot be neglected because they clearly perturb these spectra more or less strongly. In Figures 2 and 3 ($\Delta v = 1$ and 2), the

TABLE 1: Internal Coordinate Model Molecular Parameters of 2-Methylpyridine and Their Variations vs the Internal Rotation Angle of the Methyl Group (θ)

	parameters/cm^{-1}		
$\varpi_{r_{CHa}}(\theta)$	$3091.0 - 16.7\cos\theta + 20\cos 2\theta$	$\varpi_{r_{CD}}(\theta)$	$2281.0 - 11.8\cos\theta + 14.1\cos 2\theta$
$\bar{\chi}_{r_{CH}}(\theta)$	$-58.0 + 1.7\cos\theta + 1.4\cos 2\theta$	$\bar{\chi}_{r_{CD}}(\theta)$	$-30.0 + 0.9\cos\theta + 0.8\cos 2\theta$
$\lambda_{r_{CH}r_{CH}}(\theta)$	$-20.1 + 0.5\cos\theta - 1.0\cos 2\theta - 0.9\sin\theta - 1.75\sin 2\theta$	$\lambda_{r_{CH}r_{CD}}(\theta)$	$-30.15 + 0.45\cos\theta - 0.1\cos 2\theta + 0.8\sin\theta + 1.55\sin 2\theta$
$\varpi_{HCH}(\theta)$	$1356.0 - 0.75\cos\theta + 8.75\cos 2\theta$	$\varpi_{HCD}(\theta)$	$1193.0 - 0.75\cos\theta + 8.75\cos 2\theta$
$\bar{\chi}_{HCH}(\theta)$	-5.0	$\bar{\chi}_{HCD}(\theta)$	-5.0
$\varpi_{HCC}(\theta)$	$1001.0 + 10.0\cos\theta + 30.0\cos 2\theta$		
$\bar{\chi}_{HCC}(\theta)$	-5.0		
$\bar{\chi}^*_{r_{HCH}}(\theta)$	$-14.28 - 0.29\cos\theta + 1.1\cos 2\theta$	$\bar{\chi}^*_{r_{HCD}}(\theta)$	$-15.29 - 0.074\cos\theta + 0.813\cos 2\theta$
$\bar{\chi}^*_{r_{HCC}}(\theta)$	$-12.20 - 0.4\cos\theta + 0.65\cos 2\theta$		

TABLE 2: Fermi Resonance Force Constants for the CH_3 Group Corresponding to the CH Bond r_1[a]

$\alpha_i\alpha_j$	$f_{r\alpha_i\alpha_j}$/aJ Å^{-1}	$f_{rr\alpha_i\alpha_j}$/aJ Å^{-2}	$f_{rrr\alpha_i\alpha_j}$/aJ Å^{-3}
$\alpha_i\alpha_i\,(i=1,3)$	$-0.290 - 0.015\cos\theta + 0.018\cos 2\theta$	1.7	-8.7
$\alpha_i\alpha_j\,(i=1,3,j=2)$	$0.0150 - 0.0125\cos\theta + 0.0115\cos 2\theta$	-0.07	8.4
$\alpha_i\alpha_j\,(i=1,j=3)$	$0.125 + 0.013\cos\theta - 0.016\cos 2\theta$	-0.29	7.8
$\alpha_i\alpha_i\,(i=2)$	$0.020 - 0.010\cos\theta + 0.012\cos 2\theta$		
$\alpha_i\beta_j\,(i=1,3,j=1)$	$0.290 + 0.015\cos\theta - 0.018\cos 2\theta$		
$\alpha_i\beta_j\,(i=2,3,j=3)$	$0.045 - 0.020\cos\theta + 0.024\cos 2\theta$		
$\beta_i\beta_i\,(i=1)$	$-0.520 - 0.020\cos\theta + 0.024\cos 2\theta$	4.8	-17.4
$\beta_i\beta_j\,(i=1,j=2,3)$	$0.030 - 0.015\cos\theta + 0.018\cos 2\theta$		
$\beta_i\beta_i\,(i=2,3)$	$-0.030 - 0.015\cos\theta + 0.018\cos 2\theta$		

[a] The Fermi resonance force constants corresponding to the other CH bond r_2 and r_3 are deduced from circular permutations. ($r_1 = CH'_1$, $r_2 = CH'_2$, $r_3 = CH'_3$, $\alpha_1 = H_1CH_2$, $\alpha_2 = H_2CH_3$, $\alpha_3 = H_3CH_1$, $\beta_1 = H_1C_1C_2$, $\beta_2 = H_2C_1C_2$, $\beta_3 = H_3C_1C_2$).

spectra resulting from the subtraction of the aryl bands of the 2-$CD_3C_5NH_4$ are also displayed to bring out the methyl CH-stretching region.

At $\Delta v = 1$ (Figure 2), the methyl CH-stretching spectrum shows three principal bands centered at 2878, 2938, and 2983 cm^{-1}. Neglecting Fermi resonance phenomena leads to three calculated methyl CH-stretching normal modes at 2908.8 cm^{-1} (ν_s), at 2962.6 cm^{-1} ($\nu_{s'}$) and at 2994.7 cm^{-1} (ν_a) with dipole moments corresponding to A-type (μ_z), C-type (μ_y), and B-type (μ_x) vibration−rotation structures, respectively (see Table 3). Similar to toluene, disagreement between calculated and experimental spectra is ascribed also here to the occurrence of a strong Fermi resonance phenomenon. The experimental spectrum is correctly modeled by the six components calculated with the parameters displayed in Figures 1 and 2 (dashed lines in Figure 2). The two lower-frequency bands having a characteristic A-type structure are seen to result from the strong Fermi resonance between the ν_s CH-stretching mode and the δ_a and $\delta_{s'}$ overtone or combination states. The $\nu_{s'}$ and ν_a CH-stretching modes are less affected by this resonance. However, these modes, the dipole moments of which are perpendicular to the internal rotation axis, are perturbed by a Coriolis coupling induced by the internal rotation of the methyl group. The same Coriolis coupling also affects the two bands ($2\delta_a + 2\delta_{s'}$) at 2897.5 and 2849.9 cm^{-1} resulting from the Fermi resonance; it is modeled as in ref 15b. The best fit to the spectrum is obtained with a Coriolis constant $\zeta = 0.270$, a value similar to that determined for nitromethane (0.235)[15b] but lower than that of toluene (0.435).[16a] Note, however, that the present value is determined with a lower precision than the two previous ones, the higher frequency band (around 3040 cm^{-1}) resulting from this coupling being hidden by the aryl CH-stretching bands. The ζ value was thus deduced from spectra subtraction.

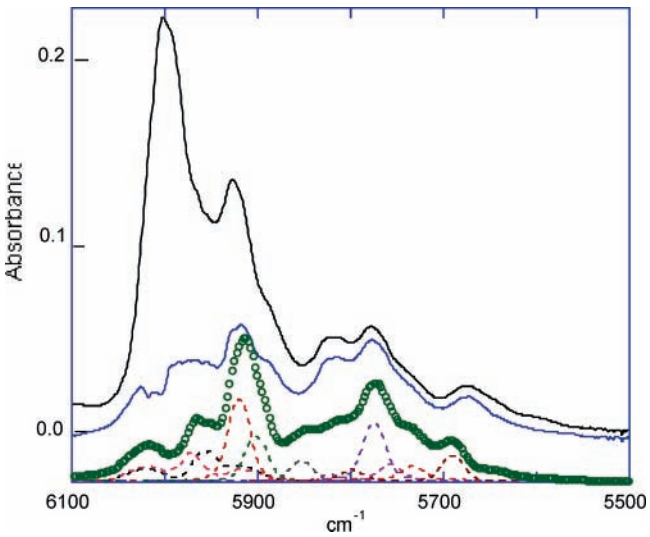

Figure 3. Experimental spectra without (offset upper solid line) and after subtraction of the aryl CH bands (middle solid line) and the calculated (circle line) spectrum in the $\Delta v = 2$ CH-stretching region of gaseous 2-$CH_3C_5NH_4$ at 298 K. The experimental spectrum is obtained by FTIR with a 4-m path-length cell, a pressure of 11 Torr, and a resolution of 1 cm^{-1}.

At $\Delta v = 2$, the calculated unperturbed spectrum consists of six methyl CH-stretching normal modes (Table 4). The three lower-frequency modes correspond to vibrations involving pure CH-stretching overtone states (e.g., $|2,0,0\rangle$), whereas the three other ones correspond to vibrations involving CH-stretching combination states (e.g., $|1,1,0\rangle$). The bands at 5888.9 and 5764.1 cm^{-1} can be assigned to symmetric modes with A-type (μ_z) vibration−rotation structure, the bands at 5953.5 and 5769.6 cm^{-1} and at 5939.8 and 5820.1 cm^{-1} to asymmetric modes with a C-type (μ_y) and B-type (μ_x) vibration−rotation structure, respectively. The experimental spectrum (Figure 3) exhibits a rather different and complex pattern. The weaker bands at 5820, 5777.5, and 5673 cm^{-1} with a poorly defined vibration−rotation profile are assigned to the methyl CH stretching. When the two strong aryl bands at 6002 and 5927 cm^{-1} are subtracted, the methyl CH-stretching region displays three other bands centered at 6025, 5970, and 5920 cm^{-1}. A strong Fermi resonance involving mainly the three HCH-bending deformations of the methyl group perturbs this region strongly. The calculated

TABLE 3: Calculated Frequencies (cm^{-1}) and Dipole Moment Components μ_x, μ_y, and μ_z (Debye) of the Fundamental Normal Mode Components of the CH_3 Methyl Group of 2-Methylpyridine[a]

υ		$\varpi_m(\theta)$	$\mu_x(\theta)$	$\mu_y(\theta)$	$\mu_z(\theta)$
1/2	$\delta_{a_{CH3}}$	$1456.6 + 1.5\cos 3\theta + 0.08\cos 6\theta$			
	$\delta_{s'_{CH3}}$	$1445.8 - 2.9\cos 3\theta - 0.65\cos 6\theta$			
	$\delta_{s_{CH3}}$	$1383.8 + 0.75\cos 3\theta + 0.07\cos 6\theta$			
	$r_{\perp_{CH3}}$	$1049.8 - 4.15\cos 3\theta + 3.84\cos 6\theta$			
	$\eta_{\parallel_{CH3}}$	$976.4 - 4.55\cos 3\theta - 0.02\cos 6\theta$			
1u	ν_a	$2994.7 - 11.8\cos 3\theta - 0.73\cos 6\theta$	$\mathbf{-4.75} - 0.9\cos 3\theta - 0.26\cos 6\theta$	$1.52\sin 3\theta + 0.45\sin 6\theta$	$\mathbf{0.4} - 1.03\cos 3\theta - 0.25\cos 6\theta$
	$\nu_{s'}$	$2962.6 + 8.6\cos 3\theta - 0.08\cos 6\theta$	$-2.69\sin 3\theta - 0.54\sin 6\theta$	$\mathbf{-6.07} + 0.56\cos 3\theta - 0.16\cos 6\theta$	$-1.44\sin 3\theta - 0.2\sin 6\theta$
	ν_s	$2908.8 + 3.3\cos 3\theta + 0.68\cos 6\theta$	$\mathbf{-1.08} + 0.83\cos 3\theta - 0.01\cos 6\theta$	$1.61\sin 3\theta + 0.01\sin 6\theta$	$\mathbf{6.18} - 0.04\cos 3\theta - 0.04\cos 6\theta$
1RF	ν_a	$3003.0 - 12.5\cos 3\theta - 0.68\cos 6\theta$	$\mathbf{4.62} + 0.95\cos 3\theta + 0.25\cos 6$	$-1.3\sin 3\theta - 0.26\sin 6\theta$	$-0.4\cos 3\theta + 1.2\cos\theta$
	$\nu_{s'}$	$2971.1 + 8.5\cos 3\theta - 0.21\cos 6\theta$	$2.54\sin 3\theta + 0.32\sin 6\theta$	$\mathbf{5.74} - 0.47\cos 3\theta + 0.19\cos 6$	$1.8\sin 3\theta + 0.23\sin 6\theta$
	ν_s	$2937.1 + 3.6\cos 3\theta + 0.65\cos 6\theta$	$0.98\cos 3\theta - 0.65\cos 6\theta$	$-1.53\sin 3\theta - 0.04\sin 6\theta$	$\mathbf{4.75} + 0.06\cos 3\theta + 0.11\cos 6$
	$2\delta_a + 2\delta_{s'}$	$2897.50 - 2.7\cos 3\theta + 0.28\cos 6\theta$	$\mathbf{0.99} + 0.03\cos 3\theta + 0.21\cos 6$	$1.52\sin 3\theta - 0.21\sin 6\theta$	$-1.2\cos 3\theta - 1.73\cos 6\theta$
	$2\delta_a + 2\delta_{s'}$	$2849.9 - 0.1\cos 3\theta + 0.01\cos 6\theta$	$-0.68\sin 3\theta + 0.25\sin 6\theta$	$\mathbf{1.76} - 0.21\cos 3\theta + 0.11\cos 6$	$-1.48\sin 3\theta + 0.51\sin 6\theta$
	$2\delta_a + 2\delta_{s'}$	$2877.7 - 2.9\cos 3\theta - 0.23\cos 6\theta$	$0.7\cos 3\theta + 0.04\cos 6\theta$	$0.12\sin 3\theta$	$\mathbf{2.8} - 0.43\cos 3\theta$

[a] The unperturbed spectrum is referred to as u and the Fermi resonance perturbed spectrum as RF.

TABLE 4: Calculated Frequencies (cm^{-1}) and Dipole Moment Components μ_x, μ_y, and μ_z (Debye) of the Stretching Normal Mode Components of the CH_3 Methyl Group of 2-Methylpyridine for the First Overtone CH-Stretching State ($\Delta v = 2$).[a]

υ		$\varpi_m(\theta)$	$\mu_x(\theta)$	$\mu_y(\theta)$	$\mu_z(\theta)$
2u	$\nu_{11s'}$	$5953.5 - 5.8\cos 3\theta - 3.7\cos 6\theta$	$0.11\sin 3\theta - 0.78\sin 6\theta$	$\mathbf{-2.62} - 0.15\cos 3\theta + 0.05\cos 6\theta$	$-1.63\sin 3\theta + 0.13\sin 6\theta$
	ν_{11a}	$5939.8 - 6.7\cos 3\theta + 4.2\cos 6\theta$	$\mathbf{2.6} - 0.13\cos 3\theta - 0.08\cos 6\theta$	$0.15\sin 3\theta - 0.81\sin 6\theta$	$\mathbf{-1.22} + 1.3\cos 3\theta + 0.35\cos 6\theta$
	ν_{11s}	$5888.9 + 9.3\cos 3\theta - 0.05\cos 6\theta$	$\mathbf{0.03} + 0.59\cos 3\theta + 0.22\cos 6\theta$	$0.43\sin 3\theta + 0.13\sin 6\theta$	$\mathbf{-4.88} - 0.5\cos 3\theta$
	$2\nu_a$	$5820.1 - 22.5\cos 3\theta - 0.3\cos 6\theta$	$\mathbf{-2.8} + 0.21\cos 3\theta + 0.02\cos 6\theta$	$1.59\sin 3\theta + 0.22\sin 6\theta$	$\mathbf{-0.08} + 1.17\cos 3\theta - 0.3\cos 6\theta$
	$2\nu_{s'}$	$5769.6 + 15.7\cos 3\theta - 7.6\cos 6\theta$	$1.06\sin 3\theta - 0.19\sin 6\theta$	$\mathbf{3.14} + 0.11\cos 3\theta + 0.8\cos 6\theta$	$1.25\sin 3\theta - 0.22\sin 6\theta$
	$2\nu_s$	$5734.1 + 10.1\cos 3\theta + 7.5\cos 6\theta$	$\mathbf{0.02} + 1.35\cos 3\theta + 0.07\cos 6\theta$	$3.4\sin 3\theta + 0.11\sin 6\theta$	$\mathbf{-4.25} + 0.14\cos 3\theta$
2RF	ϖ_1	$5972.1 - 6.1\cos 3\theta - 3.5\cos 6\theta$	$-0.07\sin 3\theta + 0.81\sin 6\theta$	$\mathbf{2.32} - 0.16\cos 3\theta - 0.1\cos 6\theta$	$1.58\sin 3\theta - 0.12\sin 6\theta$
	ϖ_2	$5959.9 - 7.1\cos 3\theta + 3.9\cos 6\theta$	$\mathbf{2.2} - 0.18\cos 3\theta - 0.1\cos 6\theta$	$0.06\sin 3\theta - 0.84\sin 6\theta$	$\mathbf{-1.13} + 1.1\cos 3\theta + 0.3\cos 6\theta$
	ϖ_3	$5920.9 - 2.6\cos 3\theta + 2.8\cos 6\theta$	$-0.77\cos 3\theta + 0.22\cos 6\theta$	$-0.19\sin 3\theta - 0.19\sin 6\theta$	$\mathbf{2.87} + 1.94\cos 3\theta$
	ϖ_4	$5901.9 + 0.9\cos 3\theta - 4.7\cos 6\theta$	$\mathbf{-1.12} - 0.081\cos 6\theta$	$0.38\sin 3\theta + 0.03\sin 6\theta$	$\mathbf{-2.17} + 1.8\cos 3\theta + 0.4\cos 6\theta$
	ϖ_5	$5871.6 + 6.8\cos 3\theta + 0.5\cos 6\theta$	$0.15\sin 3\theta$	$\mathbf{1.0} + 0.09\cos + 0.02\cos 6\theta$	$0.36\sin 3\theta + 0.07\sin 6\theta$
	ϖ_6	$5854.1 - 4.6\cos 3\theta + 2.3\cos 6\theta$	$\mathbf{0.8} - 0.6\cos 3\theta + 0.17\cos 6\theta$	$-0.04\sin 3\theta + 0.16\sin 6\theta$	$\mathbf{-1.33} - 0.9\cos 3\theta + 0.4\cos 6\theta$
	ϖ_7	$5838.0 - 8.2\cos 3\theta - 1.9\cos 6\theta$	$\mathbf{1.0} - 0.98\cos 3\theta - 0.57\cos 6\theta$	$-0.8\sin 3\theta - 0.03\sin 6\theta$	$\mathbf{-0.4} - 0.8\cos 3\theta - 0.1\cos 6\theta$
	ϖ_8	$5827.8 - 11.3\cos 3\theta - 3.0\cos 6\theta$	$\mathbf{0.2} - 0.56\cos 3\theta - 0.14\cos 6\theta$	$0.4\sin 3\theta + 0.3\sin 6\theta$	$\mathbf{1.32} - 0.4\cos 3\theta - 0.2\cos 6\theta$
	ϖ_9	$5790.6 + 13.0\cos 3\theta - 0.3\cos 6\theta$	$0.83\sin 3\theta + 0.21\sin 6\theta$	$\mathbf{1.4} - 0.6\cos 3\theta + 0.03\cos 6\theta$	$0.52\sin 3\theta - 0.38\sin 6\theta$
	ϖ_{10}	$5797.1 + 6.6\cos 3\theta - 3.5\cos 6\theta$	$0.16\sin 3\theta + 0.16\sin 6\theta$	$\mathbf{-1.1} - 1.3\cos 3\theta - 0.17\cos 6\theta$	$-0.3\sin 3\theta - 0.1\sin 6\theta$
	ϖ_{11}	$5774.1 + 7.8\cos 3\theta + 2.0\cos 6\theta$	$0.07\cos 3\theta + 0.86\cos 6\theta$	$1.43\sin 3\theta + 0.42\sin 6\theta$	$\mathbf{-2.66} - 0.2\cos 3\theta - 0.3\cos 6\theta$
	ϖ_{12}	$5764.5 + 2.5\cos 3\theta + 1.3\cos 6\theta$	$\mathbf{0.16} - 0.15\cos 3\theta + 0.14\cos 6\theta$	$-0.52\sin 3\theta + 0.2\sin 6\theta$	$\mathbf{0.87} - 1.0\cos 3\theta - 0.4\cos 6\theta$
	ϖ_{13}	$5757.4 + 2.4\cos 3\theta + 0.9\cos 6\theta$	$-0.16\sin 3\theta + 0.09\sin 6\theta$	$\mathbf{1.5} + 0.1\cos 3\theta + 0.13\cos 6\theta$	$-1.36\sin 3\theta - 0.03\sin 6\theta$
	ϖ_{14}	$5748.1 - 7.5\cos 3\theta + 2.9\cos 6\theta$	$\mathbf{0.43} - 1.0\cos 3\theta - 0.31\cos 6\theta$	$-0.82\sin 3\theta - 0.28\sin 6\theta$	$\mathbf{0.95} + 0.4\cos 3\theta + 0.4\cos 6\theta$
	ϖ_{15}	$5733.2 + 1.9\cos 3\theta + 1.1\cos 6\theta$	$0.2\sin 3\theta - 0.25\sin 6\theta$	$\mathbf{-1.38} + 0.43\cos 3\theta + 0.37\cos 6\theta$	$2.09\sin 3\theta - 0.43\sin 6\theta$
	ϖ_{16}	$5735.6 - 2.1\cos 3\theta - 2.9\cos 6\theta$	$\mathbf{-0.82} - 0.28\cos 3\theta - 0.1\cos 6\theta$	$-0.24\sin 3\theta + 0.34\sin 6\theta$	$\mathbf{0.22} + 0.9\cos 3\theta - 0.6\cos 6\theta$
	ϖ_{17}	$5722.8 - 2.5\cos 3\theta + 0.7\cos 6\theta$	$\mathbf{-0.07} + 0.15\cos 3\theta - 0.1\cos 6\theta$	$0.66\sin 3\theta + 0.38\sin 6\theta$	$\mathbf{-0.83} + 0.64\cos 3\theta - 0.02\cos 6\theta$
	ϖ_{18}	$5707.6 + 7.0\cos 3\theta - 2.2\cos 6\theta$	$0.21\sin 3\theta - 0.12\sin 6\theta$	$\mathbf{0.88} - 0.76\cos 3\theta + 0.07\cos 6\theta$	$0.21\sin 3\theta$
	ϖ_{19}	$5690.1 + 6.3\cos 3\theta + 2.3\cos 6\theta$	$\mathbf{0.04} - 0.52\cos 3\theta - 0.01\cos 6\theta$	$-1.3\sin 3\theta - 0.03\sin 6\theta$	$\mathbf{1.78} - 0.13\cos 3\theta - 0.08\cos 6\theta$

[a] The unperturbed spectrum is referred to as u and the Fermi resonance perturbed spectrum is referred to as RF; the index a and s are put by comparison with the fundamental normal modes according to their dipole moment transitions direction.

spectrum is obtained by the addition of numerous modes, the most intense of which have been displayed in Table 4 and in Figure 3 (dashed lines). The features at 6025, 5970, and 5920 cm^{-1} are mostly due to the respective ϖ_1, ϖ_2, and ϖ_3 vibrations (corresponding to the three CH-stretching combination states) affected by Fermi resonance and Coriolis coupling perturbations. The remaining part of the spectral features corresponds to a mixing of vibrations of pure CH-stretching overtone states and of CH-stretching combination states perturbed by Fermi resonance and by Coriolis coupling. Despite this complexity, a rather good agreement is found between experimental and calculated spectra (Figure 3).

Upward to $\Delta\upsilon = 3$, the CH-stretching energy can be described with a local mode basis. The calculations now yield local CH-stretching modes, and the sum over the three CH bonds can thus be ignored in eq 13. At $\Delta\upsilon = 3$, the three stronger bands at 8835, 8792, and 8717 cm^{-1} are assigned to the aryl CH-stretching overtones (Figure 4). The weaker complex spectral features centered at 8448 cm^{-1} with two shoulders at 8388 and 8530 cm^{-1} correspond to the methyl CH-stretching overtone (Figure 4). Fermi resonance phenomena involving several δ_a and $\delta_{s'}$ overtones and combination states affect this spectral region, generating several vibrational components. Because of

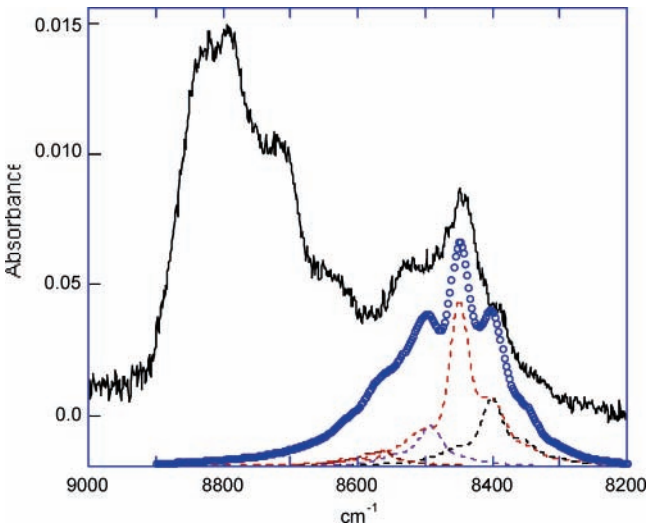

Figure 4. Experimental (solid line) and calculated (circle line) spectra of the second CH-stretching overtone ($\Delta\upsilon = 3$) of gaseous 2-$CH_3C_5NH_4$ at 298 K. The experimental spectrum is obtained by FTIR with a 4-m path-length cell, a pressure of 11 Torr, and a resolution of 2 cm^{-1}.

TABLE 5: Calculated Frequencies (cm^{-1}) and Relative Intensity Coefficient of the Local Modes of the CH_3 Methyl Group of the 2-Methylpyridine for the Second ($\Delta v = 3$), Third ($\Delta v = 4$), Fourth ($\Delta v = 5$), and Fifth ($\Delta v = 6$) Overtone CH-Stretching States.[a]

v	$\varpi_m(\theta)$	intensity (%)
3u	$8489.2 - 33.2\cos\theta + 78.1\cos 2\theta + 0.4\cos 3\theta - 0.4\cos 4\theta$	**96.8**
3RF	$8567.5 - 7.6\cos\theta + 4.1\cos 2\theta - 3.5\cos 3\theta + 0.8\cos 4\theta$	3.4
	$8564.5 + 8.0\cos\theta + 12.4\cos 2\theta + 4.4\cos 3\theta - 0.7\cos 4\theta$	3.3
	$8530.4 - 2.2\cos\theta + 6.4\cos 2\theta - 6.2\cos 3\theta + 4.5\cos 4\theta$	3.2
	$8498.1 + 0.2\cos\theta + 0.3\cos 2\theta - 0.3\cos 3\theta - 0.2\cos 4\theta$	3.0
	$8491.8 + 4.7\cos\theta + 3.8\cos 2\theta + 6.2\cos 3\theta + 2.6\cos 4\theta$	9.0
	$8455.0 - 11.3\cos\theta + 23.4\cos 2\theta + 6.6\cos 3\theta - 11.8\cos 4\theta$	**36.7**
	$8402.7 + 0.6\cos\theta + 10.3\cos 2\theta + 12.2\cos 3\theta - 7.6\cos 4\theta$	**15.2**
4u	$11079.0 - 35.1\cos\theta + 114.4\cos 2\theta + 0.1\cos 3\theta - 0.2\cos 4\theta$	**98.6**
4RF	$11241.0 - 19.2\cos\theta + 27.1\cos 2\theta + 1.5\cos 3\theta - 2.6\cos 4\theta$	3.6
	$11112.0 - 29.0\cos\theta + 59.4\cos 2\theta - 2.5\cos 3\theta + 12.2\cos 4\theta$	**23.8**
	$11168.0 - 7.4\cos\theta + 9.4\cos 2\theta + 7.6\cos 3\theta - 10.8\cos 4\theta$	5.6
	$11047.0 - 24.5\cos\theta + 75.6\cos 2\theta + 6.9\cos 3\theta - 12.6\cos 4\theta$	**55.5**
	$11028.0 + 0.04\cos\theta - 5.1\cos 2\theta + 3.0\cos 3\theta - 1.5\cos 4\theta$	5.5
5u	$13545.0 - 28.6\cos\theta + 155.8\cos 2\theta + 0.1\cos 3\theta - 0.2\cos 4\theta$	**98.9**
5RF	$13558.0 - 34.7\cos\theta + 138.1\cos 2\theta + 2.5\cos 3\theta + 1.8\cos 4\theta$	**75.8**
	$13431.0 - 19.7\cos\theta + 3.8\cos 2\theta + 0.8\cos 3\theta - 5.5\cos 4\theta$	4.4
	$13406.0 - 19.0\cos\theta + 5.8\cos 2\theta - 11.5\cos 3\theta - 6.0\cos 4\theta$	16.0
6u	$15887.0 - 12.7\cos\theta + 201.7\cos 2\theta + 0.1\cos 3\theta - 0.2\cos 4\theta$	**99.6**
6RF	$16036.0 - 66.9\cos\theta + 49.8\cos 2\theta - 3.7\cos 3\theta + 1.3\cos 4\theta$	5.0
	$16074.0 - 29.7\cos\theta + 8.0\cos 2\theta + 0.1\cos 3\theta + 2.3\cos 4\theta$	3.4
	$15956.0 - 43.9\cos\theta + 78.6\cos 2\theta + 6.2\cos 3\theta - 3.7\cos 4\theta$	7.4
	$15877.0 + 4.3\cos\theta + 87.8\cos 2\theta + 8.4\cos 3\theta - 11.7\cos 4\theta$	**22.1**
	$15875.0 - 1.9\cos\theta + 171.7\cos 2\theta + 10.2\cos 3\theta - 33.3\cos 4\theta$	**51.1**
	$15790.0 + 14.9\cos\theta + 49.2\cos 2\theta + 16.5\cos 3\theta - 12.4\cos 4\theta$	**10.2**

[a] The unperturbed spectrum is referred to as u and the Fermi resonance perturbed spectrum is referred to as RF.

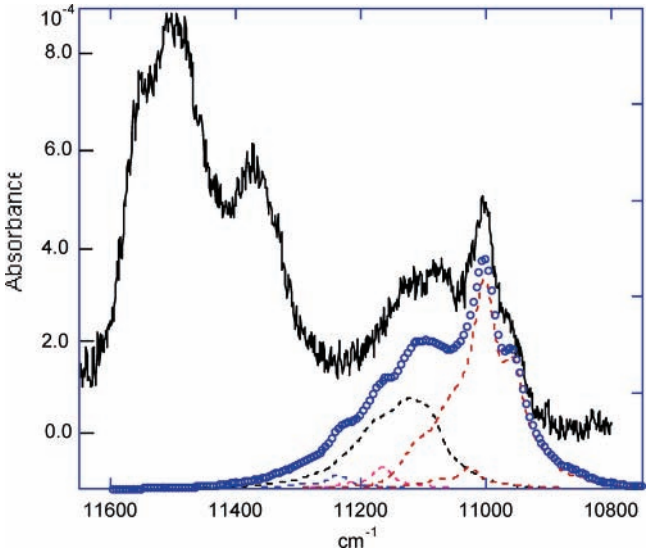

Figure 5. Experimental (solid line) and calculated (circle line) spectra of the third CH-stretching overtone ($\Delta v = 4$) of gaseous 2-$CH_3C_5NH_4$ at 298 K. The experimental spectrum is obtained by FTIR with a 4-m path-length cell, a pressure of 11 Torr, and a resolution of 2 cm^{-1}.

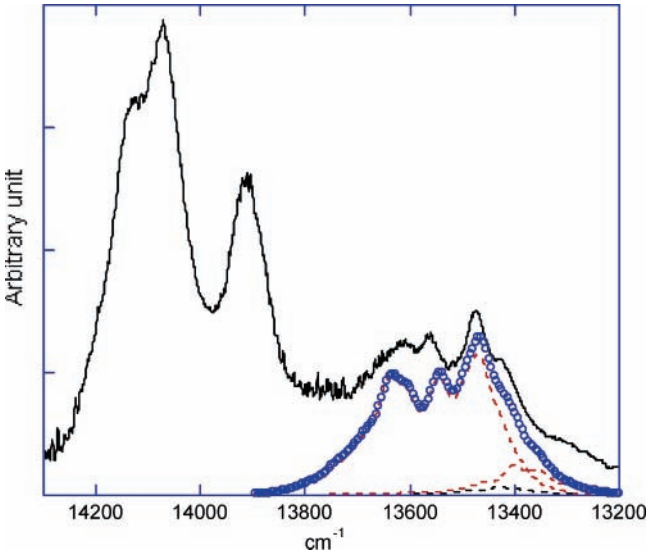

Figure 6. Experimental (solid line) and calculated (circle line) spectra of the fourth CH-stretching overtone ($\Delta v = 5$) of gaseous 2-$CH_3C_5NH_4$ at 310 K. The experimental spectrum is obtained photoacoustically with an 11-cm path-length cell and a pressure of 23 Torr.

the lower symmetry of this system compared to toluene, the vibrational energy is more widely spread. The use of the diabatic rotation technique allows disentangling of the several avoided crossings of these perturbed modes along the θ variation. The so obtained 30 ϖ_m components are summed up to obtain the reconstructed spectrum (Figure 4) (the most intense bands are displayed in Table 5 and in Figure 4 (dashed lines)).

At $\Delta v = 4$, in addition to the three strong aryl CH-stretching bands centered at 11 570, 11 510, and 11 383 cm^{-1}, the spectrum exhibits a group of weaker bands at 11 136, 11 090 and 11 011 cm^{-1}, with a shoulder at 10 979 cm^{-1} assigned to the methyl CH-stretching modes (Figure 5). Fermi resonance phenomena are still present, but the frequency domain of the unperturbed CH-stretching band is intermediate between that of the states involved in resonance phenomena. This leads to offsets of the resonant effects of varying importance. The overtone spectral feature is thus slightly affected. The calculated spectrum is the sum of about 20 calculated bands (the most intense ones are displayed in Table 5 and in Figure 5 (dashed lines)).

At $\Delta v = 5$, the spectrum displays three strong aryl CH-stretching bands centered at 14 140, 14 093 and 13 926 cm^{-1}, a more or less regular triplet structure at 13 617, 13 564, and 13 475 cm^{-1}, as expected for the unperturbed methyl CH-stretching spectral profile and a broad shoulder at 13 425 cm^{-1} (Figure 6). Here, the calculations indicate that the perturbation due to Fermi resonance becomes negligible. The calculated spectral profile is mostly due to one component (dashed line in Figure 6), very similar to that obtained for the unperturbed case

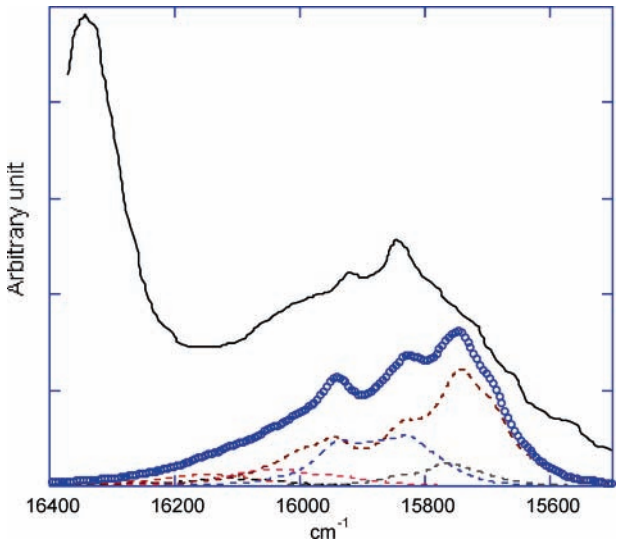

Figure 7. Experimental (solid line) and calculated (circle line) spectra of the fifth CH-stretching overtone ($\Delta v = 6$) of gaseous 2-$CH_3C_5NH_4$ at 310 K. The experimental spectrum is obtained photoacoustically with an 11-cm path-length cell and a pressure of 23 Torr.

but shifted toward higher frequencies. This blue-shift, attributable to Fermi resonances involving essentially HCH and HCC angle deformation combination states, cannot be reproduced by considering only the internal rotation coupling.[24b] Fermi resonance also gives rise to a weak band on the low-frequency side of the spectrum that corresponds approximately to the shoulder observed in the experimental spectrum. A similar weak Fermi resonance perturbation is found at this energy for toluene.[16a] Thus, at this energy, the comparison of the spectral features of toluene and of 2-methylpyridine reveals the part attributable to the difference in the rotational potential of the methyl group of the two molecules.

At $\Delta v = 6$, the methyl CH-stretching spectrum exhibits a more embedded feature with a principal maximum at 15 850 cm^{-1} and three shoulders at 15 745, 15 930, and 16 040 cm^{-1} (Figure 7). The unperturbed spectrum would show a triplet structure very similar to that observed for the fourth overtone (Figure 6) (Table 5). The difference observed between the unperturbed and the experimental spectral profiles demonstrates the occurrence of non-neglible Fermi resonance phenomena. Indeed, because of a closer frequency matching between the combination states involving HCH and HCC angle deformation combinations and the CH-stretching overtone states, Fermi resonance phenomena become more efficient, inducing a complicated splitting of the unperturbed overtone stretching state (Table 5). Unfortunately, the calculation of this overtone spectrum cannot be carried out completely because of the size of the Hamiltonian matrix, which becomes exceedingly large if all the tiers are introduced. In addition, even when only 4 tiers are considered in the calculation, the intensities and the frequencies of the calculated states are so widely spread that the technique of diabatic rotations is no longer efficient to disentangle the complex set of calculated states. Thus, the reconstructed spectrum affords only an approximated feature of the experimental one.

(b) CHD_2 Derivative. Figures 8−10 show the experimental and calculated CH-stretching overtone spectra of gaseous 2-CHD_2-6DC_5NH_3 at $\Delta v = 3$ and 4 and of gaseous 2-$CHD_2C_5NH_4$ at $\Delta v = 5$. Several experimental 2-$CHD_2C_5NH_4$ spectra were previously recorded from $\Delta v = 1-4$.[17c] The first overtone spectra ($\Delta v = 1-3$) were well reproduced by considering only the coupling of the CH-stretching mode with the internal rotation of the methyl group, showing that, in this case, the Fermi resonance coupling does not strongly disturb the spectral pattern up to $\Delta v = 3$.

In the present more complete treatment, a fairly good agreement between the calculated and the experimental spectra is obtained with the parameters set used for the calculation of the CH_3 group (Tables 1 and 2). The increasing shift of the isolated CH-stretching spectra toward higher frequencies as excitation increases is due to anharmonic Fermi resonance coupling with HCD bending modes, as evidenced by comparing the unperturbed and perturbed calculated spectra (Table 6). This coupling begins to be detectable from the second overtone spectrum, as it gives rise to a weak feature around 8300 cm^{-1} assigned to combination states involving HCD deformation modes (Figure 8). Apart from the stronger aryl CH-stretching band centered at 8815 cm^{-1}, the other bands of the spectrum at 8526 and 8475 cm^{-1} with their two shoulders at 8430 and 8580 cm^{-1}, respectively, are due to the almost unperturbed methyl CH-stretching modes.

With increasing energy, the combination states involving HCD deformation modes come closer to resonance. At $\Delta v = 4$, the spectrum exhibits a strong band at 11 457 cm^{-1} with a shoulder at 11 476 cm^{-1} assigned to the aryl CH-stretching overtones. The complex structure with four maxima at 11 201, 11 130, 11 053, and 11 020 cm^{-1} and a shoulder at 10 880 cm^{-1} is due to the methyl CH-stretching modes (Figure 9). It is well reproduced by the calculation. Most of the calculated spectral profile arises from two principal components (dashed lines in Figure 9) resulting from the splitting of the unperturbed stretching vibration in Fermi resonance with combination states involving HCD deformation modes (Table 6).

At $\Delta v = 5$, the spectrum shows three strong bands at 14 137, 14 093, and 13 926 cm^{-1} assigned to the aryl CH-stretching modes of the perhydrogenated pyridine ring. The weaker main band with three maxima at 13 492, 13 616, and 13 675 cm^{-1} and the shoulder at 13 410 cm^{-1} are due to the methyl CH-stretching modes (Figure 10). At this high level of CH bond excitation, the CH−CD interbond coupling becomes efficient, inducing an extra structure attributable to the (4νCH + νCD) combination states at the low-frequency side of the unperturbed spectrum (Table 6). Indeed, the "tuning" of these interactions into resonance at high levels of CH bond excitation is due to the anharmonicity difference of the CH and CD bonds. This interaction generally causes a further blue-shift of the CH-stretching frequency in partially deuterated species compared to hydrogenated molecules as excitation increases. However, this blue-shift is reduced by Fermi resonance phenomena involving HCD deformation combinations. The calculated spectral profile, which shows two principal components (dashed lines in Figure 10), is in good agreement with the experimental one (Table 6).

Because of the lack of a deuterated compound, we have not been able to record the $\Delta v = 6$ spectrum.

V. Conclusion

The experimental CH-stretching overtone spectra of the low hindered rotating methyl group of gaseous 2-CH_3 (from $\Delta v = 1-6$) and 2-CHD_2 (from $\Delta v = 1-5$) have been recorded and successfully simulated. The theoretical model used takes into account, within the adiabatic approximation, the coupling of the anharmonic CH stretch with the internal rotation of the methyl group and with isoenergetic combination states involving angle deformation modes of the methyl group. The description of the vibrational system in terms of redundant internal

TABLE 6: Calculated Frequencies (cm^{-1}) of the Angles Deformation Modes and of the local mode CH-stretching states (calculated from $v = 1$ to $\Delta v = 5$ with their Relative Intensity Coefficient) of the CHD_2 Methyl Group of the 2-Methylpyridine

v	$\varpi_m(\theta)$	intensity
δ_{CHD}	$1306.3 + 4.6 \cos\theta + 8.4 \cos 2\theta$	
δ_{CHD}	$1284.6 - 1.5 \cos\theta - 3.5 \cos 2\theta$	
δ_{CD_2}	$1049.9 + 5.5 \cos\theta + 16.2 \cos 2\theta$	
$r_{\perp CH_2}$	$885.6 - 5.4 \cos\theta - 23.4 \cos 2\theta$	
$r_{\parallel CH_2}$	$832.1 - 1.5 \cos\theta + 2.7 \cos 2\theta$	
1u	$2956.5 - 15.2 \cos\theta + 23.75 \cos 2\theta$	**0.998**
1RF	$2961.9 - 15.5 \cos\theta + 24.4 \cos 2\theta$	**0.993**
2u	$5790.9 - 27.2 \cos\theta + 50.5 \cos 2\theta$	**0.996**
2RF	$5802.6 - 22.6 \cos\theta + 54.6 \cos 2\theta$	**0.978**
3u	$8503.4 - 34.4 \cos\theta + 80.9 \cos 2\theta$	**0.993**
	$8528.3 - 36.1 \cos\theta + 82.2 \cos 2\theta$	**0.941**
3RF	$8327.5 - 38.2 \cos\theta + 48.7 \cos 2\theta$	0.270
4u	$11094 - 35.4 \cos\theta + 115.5 \cos 2\theta$	**0.985**
4RF	$11147.0 - 40.8 \cos\theta + 110.9 \cos 2\theta$	**0.782** $- 0.016 \cos\theta + 0.07 \cos 2\theta$
	$11070.0 - 27.5 \cos\theta + 102.5 \cos 2\theta$	0.199
	$11028.0 - 41.7 \cos\theta + 84.8 \cos 2\theta$	**0.514** $- 0.1 \cos 2\theta$
5u	$13565 - 28.8 \cos\theta + 154.6 \cos 2\theta$	0.967
	$13254 - 31.3 \cos\theta + 109.7 \cos 2\theta$	0.244
5RF	$13724 - 47.1 \cos\theta + 111.7 \cos 2\theta$	$0.26 + 0.105 \cos 2\theta$
	$13689 - 39.8 \cos\theta + 115.6 \cos 2\theta$	$0.133 + 0.168 \cos\theta + 0.122 \cos 2\theta$
	$13590 - 40.5 \cos\theta + 131.9 \cos 2\theta$	**0.741**
	$13449 - 45.7 \cos\theta + 92.5 \cos 2\theta$	**0.360** $- 0.153 \cos 2\theta$

[a] The unperturbed spectrum is referred to as u and the Fermi resonance perturbed spectrum is referred to as RF.

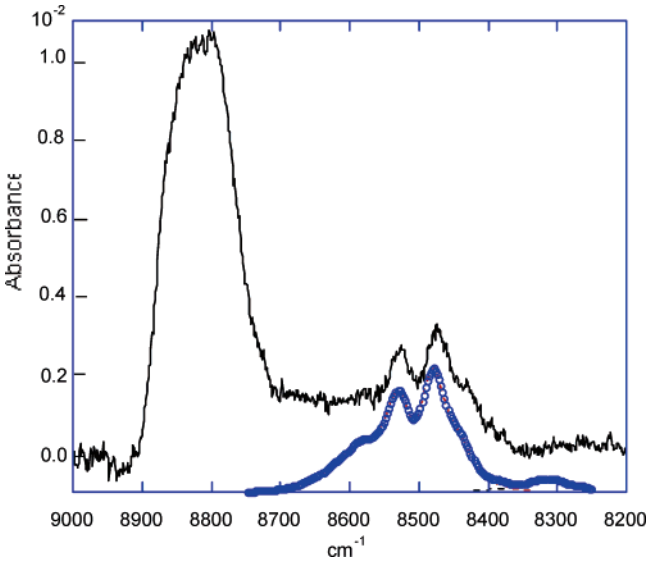

Figure 8. Experimental (solid line) and calculated (circle line) spectra of the second CH-stretching overtone ($\Delta v = 3$) of gaseous 2-CHD_2,-6DC_5NH_3 at 298 K. The experimental spectrum was obtained by FTIR with a 4-m path-length cell, a pressure of 11 Torr, and a resolution of 2 cm^{-1}.

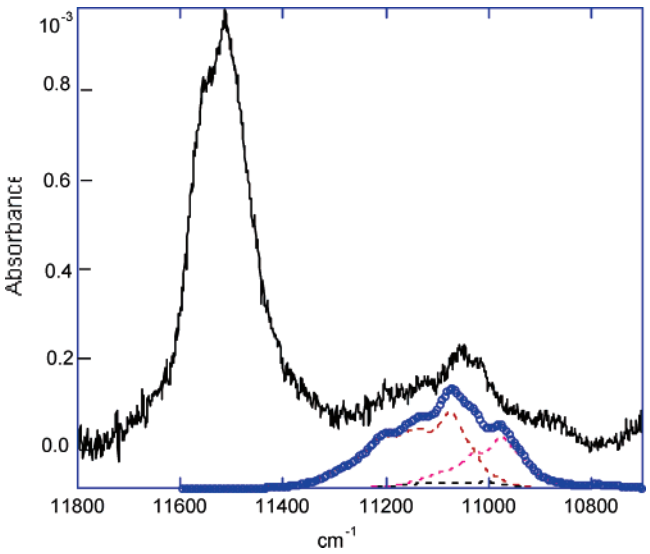

Figure 9. Experimental (solid line) and calculated (circle line) spectra of the third CH-stretching overtone ($\Delta v = 4$) of gaseous 2-CHD_2,-6DC_5NH_3 at 298 K. The experimental spectrum was obtained by FTIR with a 4-m path-length cell, a pressure of 11 Torr, and a resolution of 2 cm^{-1}.

coordinates in the unambiguous canonical form has the advantage of allowing a simultaneous analysis of isotopic derivatives with different symmetry and to offer a clear physical picture of intramolecular vibrational energy redistribution.

Furthermore, to test the transferrability between parent molecules of the Fermi resonance parameters, we have used the set of coupling parameters previously determined by a simultaneous fit to the experimental overtone spectra (from $\Delta v = 1$ to 6) of three isotopic derivatives of toluene (that is to say 18 spectra).[16] The other parameters are determined by ab initio methods and spectroscopically scaled.

At low energy ($\Delta v = 1$ and 2), the coupling between the three CH bonds of the CH_3 methyl group is strong enough to generate nonrotating normal modes which are in turn perturbed by strong Fermi resonances with combination states involving HCH angle deformation modes. Coriolis coupling induced by internal rotation further perturbs the vibrational modes perpendicular to the rotational axis as found earlier for toluene[16] and nitromethane.[15]

At higher energy, the description in local mode basis becomes relevant. Because of the lower symmetry of the 2-methylpyridine system, the perturbed vibrational patterns along the internal rotation coordinate become more complex and dense than those of toluene at the same energy. The technique of the diabatic rotations is used to disentangle the numerous avoided crossings in these vibrational patterns. The perturbations due to the Fermi resonance phenomena involving HCH angle deformations vanish progressively up to $\Delta v = 5$. At this energy, the spectrum is almost unperturbed. At $\Delta v = 6$, an important vibrational redistribution takes place again, now essentially related to Fermi resonance phenomena involving combination states of HCH and HCC angle deformations. The high density and the complexity

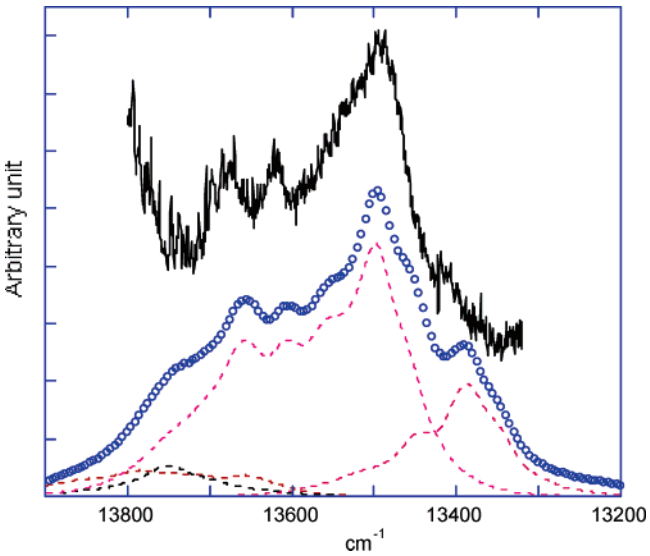

Figure 10. Experimental (solid line) and calculated (circle line) spectra of the fourth CH-stretching overtone ($\Delta v = 5$) of gaseous 2-$CHD_2C_5NH_4$ at 310 K. The experimental spectrum was obtained photoacoustically with an 11-cm path-length cell and a pressure of 23 Torr.

of the involved vibrational states prevent a good simulation of this spectrum.

In the CHD_2 compound, the CH−CD interbond coupling induces a blue-shift of the overtone spectra and the appearance of additional features in the high-energy overtone spectra corresponding to $[(n-1)\nu CH + 1\nu CD]$ resonant combination states. This shift progressively increases up to $\Delta v = 4$, attributable to Fermi resonance phenomena involving mainly HCD bending modes. The "tuning" of these interacting states into resonance is reached at $\Delta v = 5$ and causes strong intramolecular vibrational energy redistribution.

The different overtone spectra are affected to various extents by Fermi resonances, depending on the frequency matching of the bright states with the isoenergetic resonant states. In some cases, the improvement brought by this study may appear moderate for some of these spectra as compared with the previous ones that only consider the coupling with the internal rotation.[17,24] Nevertheless, taking into account all the most important couplings allows modeling of the spectra of several isotopic derivatives by using the same parameters. Actually, this set of parameters may not be unique, but it succeeds in the simultaneous reconstruction of the CH-stretching overtone spectra of two isotopic derivatives of 2-methylpyridine from $\Delta v = 1-6$ and in the parametrization of the Fermi resonance couplings of a rotating methyl chromophore for two parent molecules, picoline and toluene.

As already observed in toluene, the CH_3 and the CHD_2 chromophores are differently affected by IVR. Efficient IVR only affects the CH-stretching spectra of the CHD_2 group at relatively high energy ($\Delta v = 5$) whereas, for the CH_3 group, strong IVR occurs in limited energy domains ($\Delta v = 1$, 2, and 6).

The slight differences observed between the spectral features of toluene and 2-methylpyridine could be due to differences brought about by the molecular environment. The differences of symmetry and height of the hindering potential have only subtle effects on the strength and location of the IVR processes of the rotating methyl group.

In conclusion, we have shown that Fermi resonance coupling parameters can be transferred for the calculation of overtone spectra of molecules possessing a similar chromophore. In complex molecular systems where ab initio results often cannot be obtained (or with large quantitative errors), this could offer a possibility for a first rough analysis of the IVR phenomena.

Acknowledgment. We thank J.C. Leicknam for the calculation of the gaseous rotation-vibration profiles.

References and Notes

(1) Gruebele, M. *Adv. Chem. Phys.* **2000**, *114*, 193; Callegary, A.; Pearman, R.; Choi, S.; Engels, P.; Srivastava, H.; Gruebele, M.; Lehmann, K. K.; Scoles, G. *Mol. Phys.* **2003**, *101*, 551.

(2) Quack, M. *Annu. Rev. Phys. Chem.* **1990**, *41*, 839; *J. Mol. Struct.* **1993**, *292*, 171; Quack, M.; Kutzelnigg, W. *Ber. Bunsen-Ges. Phys. Chem.* **1995**, *99*, 231 and refs therein.

(3) Crim, F. F. *Annu. Rev. Phys. Chem.* **1993**, *44*, 397; *J. Phys. Chem.* **1996**, *100*, 12725 and refs therein; *J. Phys. Chem.* **2004**, *120*, 6973.

(4) Lehman, K. K.; Pates, B. H.; Scoles, G. *Ann. Rev. Phys. Chem.* **1994**, *45*, 241 and refs. therein; Dolce, J. W.; Callegari, A.; Meyer, B.; Lehman, K. K.; Scoles, G. J. *Phys. Chem.* **1997**, *107*, 6549.

(5) Nesbitt, D. J.; Field, R. W. *J. Phys. Chem.* **1996**, *100*, 12735 and refs therein.

(6) Henry, B. R. *Acc. Chem. Res.* **1987**, *20*, 429 and refs therein.

(7) Luckaus, D.; Quack, M. *Chem. Phys. Lett.* **1992**, *190*, 581; Luckaus, D.; Quack, M. *Chem. Phys. Lett.* **1993**, *205*, 277.

(8) Palmieri, P.; Tarroni, R.; Hühn, M. M.; Handy, N. C.; Willetts, A. *Chem. Phys.* **1995**, *190*, 327.

(9) Marquardt, R.; Sanchez Gonçalves, N.; Sala, O. *J. Chem. Phys.* **1995**, *103*, 8391.

(10) Law, M. M. *J. Chem. Phys.* **1999**, *111*, 10021.

(11) Chen, X.; Melchior, A.; Bar, I.; Rosenwaks, S. *J. Chem. Phys.* **2000**, *112*, 4111.

(12) Quack, M.; Willeke, M. *J. Chem. Phys.* **1999**, *110*, 11958.

(13) Boyarkin, O. V.; Lubich, L.; Settle, R. D. F.; Perry, D. S.; Rizzo, T. R. *J. Chem. Phys.* **1997**, *107*, 8409; Boyarkin, O. V.; Rizzo, T. R.; Perry, D. S. *J. Chem. Phys.* **1999**, *110*, 11346; Boyarkin, O. V.; Rizzo, T. R.; Perry, D. S. *J. Chem. Phys.* **1999**, *110*, 11359.

(14) (a) Halonen, L. *J. Chem. Phys.* **1997**, *106*, 831. (b) Halonen, L. *J. Chem. Phys.* **1997**, *106*, 7931. (c) Hänninen, V.; Horn, M.; Halonen, L. *J. Chem. Phys.* **1999**, *111*, 3018.

(15) (a) Cavagnat, D.; Lespade, L.; Lapouge, C. *J. Chem. Phys.* **1995**, *103*, 10502. (b) Cavagnat, D.; Lespade, L. *J. Chem. Phys.* **1997**, *106*, 7946. (c) Cavagnat, D.; Lespade, L. *J. Chem. Phys.* **1998**, *108*, 9275.

(16) (a) Cavagnat, D.; Lespade, L. *J. Chem. Phys.* **2001**, *114*, 6030. (b) Cavagnat, D.; Lespade, L. *J. Chem. Phys.* **2001**, *114*, 6041.

(17) (a) Cavagnat, D.; Lautié, M. F. *J. Raman Spectrosc.* **1990**, *21*, 185. (b) Lapouge, C.; Cavagnat, D. *J. Phys. Chem. A* **1998**, *102*, 8393. (c) Bergeat, A.; Cavagnat, D.; Lapouge, C.; Lespade, L. *J. Phys. Chem. A* **2000**, *104*, 9233.

(18) Bethardy, G. A.; Wang, X.; Perry, D. S. *Can. J. Chem.* **1994**, *72*, 652 and refs therein.

(19) McLlroy, A.; Nesbitt, D. J. *J. Chem. Phys.* **1994**, *101*, 3421.

(20) Cavagnat, D.; Lascombe, J. *J. Mol. Spectrosc.* **1982**, *92*, 141.

(21) Martens, C. C.; Reinhardt, W. P. *J. Chem. Phys.* **1990**, *93*, 5621.

(22) Anastasakos, L.; Wildman, T. A. *J. Chem. Phys.* **1993**, *99*, 9453.

(23) (a) Sowa, M. G.; Henry, B. R. *J. Chem. Phys.* **1991**, *95*, 3040. (b) Kjaergaard, H. G.; Turnbull, D. M.; Henry, B. R. *J. Phys. Chem.* **1997**, *101*, 2589. (c) Zhu, C.; Kjaergaard, H. G.; Henry, B. R. *J. Chem. Phys.* **1997**, *107*, 691; Kjaergaard, H. G.; Turnbull, D. M.; Henry, B. R. *J. Phys. Chem.* **1998**, *102*, 6095. (d) Kjaergaard, H. G.; Rong, Z.; McAlees, A. J.; Howard, D.; Henry, B. R. *J. Phys. Chem. A* **2000**, *104*, 6398. (e) Rong, Z.; Zhu, C.; Henry, B. R. *J. Phys. Chem. A* **2003**, *107*, 10771.

(24) (a) Proos, R. J.; Henry, B. R. *J. Phys. Chem. A* **1999**, *103*, 8762. (b) Rong, Z.; Kjaergaard, H. G.; Henry, B. R. *J. Phys. Chem. A* **2002**, *106*, 4368. (c) Rong, Z.; Howard, D. L.; Kjaergaard, H. G. *J. Phys. Chem. A* **2003**, *107*, 4607.

(25) (a) Moss, D. B.; Parmenter, C. S. *J. Chem. Phys.* **1993**, *98*, 6897. (b) Timbers, P. J.; Parmenter, C. S.; Moss, D. B. *J. Chem. Phys.* **1994**, *100*, 1028. (c) Zhao, Z. Q.; Parmenter, C. S. *J. Chem. Phys.* **1995**, *99*, 536.

(26) (a) Lespade, L.; Rodin, S.; Cavagnat, D.; Abbate, S. *J. Phys. Chem.* **1993**, *97*, 6134. (b) Rodin-Bercion, S.; Cavagnat, D.; Lespade, L.; Maraval, P. *J. Phys. Chem.* **1995**, *99*, 3005. (c) Lespade, L.; Rodin-Bercion, S.; Cavagnat, D. *J. Phys. Chem. A* **1997**, *101*, 2568.

(27) (a) Green, J. H. S.; Kynaston, W.; Paisley, H. M. *Spectrochim. Acta* **1963**, *19*, 549. (b) Lamba, O. P.; Parihan, J. S.; Bist, H. D.; Jain, Y. S. *Indian J. Pure Appl. Phys.* **1983**, *21*, 236. (c) Bini, R.; Foggi, P.; Della Valle, R. G. *J. Phys. Chem.* **1991**, *95*, 3027. (d) Lopez Tocon, I.; Wolley, M. C.; Otero, J. C.; Marcos, J. I. *J. Mol. Struct.* **1998**, *470*, 241. (e) Arenas,

J. F.; Lopez Tocon, I.; Otero, M. C.; Marcos, J. I. *J. Mol. Struct.* **1999**, *476*, 139.

(28) Rudolph, H. D.; Dreizler, H.; Jaeschke, A.; Wendling, P. *Z. Naturforsch. A* **1967**, *22*, 940.

(29) Hollas, J. M. *Recent Experimental and Computational Advances in Molecular Spectroscopy;* Kluwer Academic Publishers: Netherlands, **1993**, pp 27−61; Zhu, Q. S.; Campargue, A.; Stoeckel, F. *Spectrochim. Acta A* **1994**, *50*, 663.

(30) Vasquez, J.; Lopez Gonzalez, J. J.; Marquez, F.; Martinez Torres, E.; Boggs, J. E. *J. Phys. Chem. A* **2001**, *105*, 9354.

(31) Martinez Torres, E.; Lopez Gonzalez, J. J.; Fernandez Gomez, M. *J. Chem. Phys.* **1999**, *110*, 3302; Martinez Torres, E.; Lopez Gonzalez, J. J.; Vasquez Quesada, J. *J. Mol. Struct.* **2004**, *705*, 141.

(32) Wilson, E. B., Jr.; Decius, J. C.; Cross, P. C. *Molecular Vibrations;* McGraw-Hill: NY, **1955**.

(33) (a) Fehrensen, B.; Luckhaus, D.; Quack, M. Z. *Phys. Chem. (Munich)*, **1999**, *209*, 1. (b) Luckhaus, D. *J. Chem. Phys.* **2000**, *113*, 1329.

(34) Guissani, Y.; Leicknam, J. C.; Bratos, S. *Phys. Rev. A* **1977**, *16*, 2072; Leicknam, J. C.; Guissani, Y.; Bratos, S. *Phys. Rev. A* **1980**, *21*, 1005; Leicknam, J. C. *Phys. Rev. A* **1980**, *22*, 2286.